Identification and Characterization of Allophenylnorstatine-Based Inhibitors of Plasmepsin II, an Antimalarial Target†

Azin Nezami,‡ Irene Luque,‡ Tooru Kimura,§ Yoshiaki Kiso,§ and Ernesto Freire*,‡

Department of Biology and The Johns Hopkins Malaria Research Institute, The Johns Hopkins University, Baltimore, Maryland 21218, and Department of Medicinal Chemistry, Center for Frontier Research in Medicinal Science, Kyoto Pharmaceutical University, Yamashina-ku, Kyoto 607-8412, Japan

Received September 4, 2001; Revised Manuscript Received December 13, 2001

ABSTRACT: Plasmepsin II is a key enzyme in the life cycle of the *Plasmodium* parasites responsible for malaria, a disease that afflicts more than 300 million individuals annually. Since plasmepsin II inhibition leads to starvation of the parasite, it has been acknowledged as an important target for the development of new antimalarials. In this paper, we identify and characterize high-affinity inhibitors of plasmepsin II based upon the allophenylnorstatine scaffold. The best compound, KNI-727, inhibits plasmepsin II with a K_i of 70 nM and a 22-fold selectivity with respect to the highly homologous human enzyme cathepsin D. KNI-727 binds to plasmepsin II in a process favored both enthalpically and entropically. At 25 °C, the binding enthalpy (ΔH) is −4.4 kcal/mol and the entropic contribution ($-T\Delta S$) to the Gibbs energy is −5.56 kcal/mol. Structural stability measurements of plasmepsin II were also utilized to characterize inhibitor binding. High-sensitivity differential scanning calorimetry experiments performed in the absence of inhibitors indicate that, at pH 4.0, plasmepsin II undergoes thermal denaturation at 63.3 °C. The structural stability of the enzyme increases with inhibitor concentration in a manner for which the binding energetics of the inhibitor can quantitatively account. The effectiveness of the best compounds in killing the malaria parasite was validated by performing cytotoxicity assays in red blood cells infected with *Plasmodium falciparum*. EC_{50}s ranging between 6 and 10 μM (3−6 μg/mL) were obtained. These experiments demonstrate the viability of the allophenylnorstatine scaffold in the design of powerful and selective plasmepsin inhibitors.

Malaria is one of the most serious infectious diseases in the world, affecting more than 300 million individuals each year. It has been estimated that approximately 40% of the world's population lives in regions where malaria is endemic. Each year between 1 and 1.5 million people, mainly children, die from malaria, a number that is continuously increasing due to the proliferation of parasites that are resistant to conventional drug therapies (*1*). The rapid spread of drug resistant parasites clearly underscores the need for new therapies and consequently the identification of novel targets for drug development. The malaria parasite uses the hemoglobin of the infected victim as a source of nutrients and energy. One of the key enzymes involved in the degradation of hemoglobin is the aspartic protease plasmepsin II. Since the inhibition of this enzyme leads to starvation of the parasite, plasmepsin II has been acknowledged as an important target for the development of new antimalarial drugs (*2*).

Four species of protozoan parasites of the genus *Plasmodium* (*Plasmodium falciparum*, *Plasmodium vivax*, *Plasmodium malariae*, and *Plasmodium ovale*) are responsible for malaria in humans. *P. vivax* is the most common species, but *P. falciparum* causes the most fatalities (*3*, *4*). The *Plasmodium* parasite invades red blood cells and consumes up to 75% of their hemoglobin content (*5*). Hemoglobin degradation takes place in an acidic digestive vacuole in the parasite. The digestive vacuoles are acidic single-membrane organelles with an internal pH between 4 and 5.4 (*2*). Three enzymes that digest hemoglobin have been identified in the food vacuole, one cysteine protease (falcipain) and two aspartic proteases (plasmepsin I and plasmepsin II) (*2*). The inhibition of any of these enzymes leads to the starvation of the parasite and has been proposed as a viable strategy for drug development (*2*). The sequences of plasmepsin I and plasmepsin II are 73% identical. They have somewhat similar substrate specificities, and both contribute to the degradation of hemoglobin. Plasmepsin I is synthesized and processed to a mature form soon after the parasite invades the red blood cell, while the appearance of plasmepsin II occurs later in development (*6*). Plasmepsin II can be efficiently expressed in *Escherichia coli*, and its high-resolution structure has been determined by X-ray crystallography (*7*, *8*), making it the target of choice for structure-based drug design.

Plasmepsin II is a protein of 37 kDa (329 amino acids). The crystallographic structure of plasmepsin II in complex with the generic statine-based aspartic protease inhibitor pepstatin A (IvaValValStaAlaSta) has been obtained at 2.7

† Supported by National Institutes of Health Grants GM 51362 and GM 57144 and National Science Foundation Grant MCB-9816661. I.L. was a recipient of a postdoctoral fellowship from the Fundacion Ramon Areces (Madrid, Spain).

* To whom correspondence should be addressed. Phone: (410) 516-7743. Fax: (410) 516-6469. E-mail: ef@jhu.edu.

‡ The Johns Hopkins University.

§ Kyoto Pharmaceutical University.

10.1021/bi0117549 CCC: $22.00
Published on Web 01/26/2002

Å for the *P. falciparum* enzyme (PDB entry 1sme) (*8*) and 2.5 Å for the *P. vivax* enzyme (PDB entry 1qs8). Plasmepsin II has the typical bilobal structure and topology of eukaryotic aspartic proteases. The active site is located at the interface between the two lobes and is partially covered by a characteristic β-hairpin structure known as the flap. The secondary structure of plasmepsin II is predominantly β-sheet with only a small fraction ($\sim$10%) of amino acids in α-helix. Even though pepstatin A and other related statine-containing peptides are known to inhibit plasmepsin II and other aspartic proteases, very few nonpeptidic inhibitors have been described. A common problem with these inhibitors is their poor selectivity and discrimination versus the human aspartic protease cathepsin D. Cathepsin D is a human protease in the endosomal−lysosomal pathway involved in lysosomal biogenesis and protein targeting. Its overall sequence is 35% homologous with that of plasmepsin II, and the level of binding site homology is even higher, thus representing a target that needs to be avoided in the development of plasmepsin II inhibitors.

Allophenylnorstatine-based compounds have been described previously in relation to the development of HIV-1 protease inhibitors (*9*−*14*). These compounds are characterized as containing a unique unnatural amino acid, allophenylnorstatine [(2*S*,3*S*)-3-amino-2-hydroxy-4-phenylbutyric acid] containing a hydroxymethylcarbonyl isostere. Some of these compounds have been shown to be high-affinity inhibitors of the HIV-1 protease; they have low toxicity and excellent bioavailability (*9*−*14*). Here we describe several allophenylnorstatine-based compounds that exhibit powerful and selective inhibition of plasmepsin II. Furthermore, these compounds are highly effective in killing the malaria parasite in infected human erythrocyte-based assays.

MATERIALS AND METHODS

Plasmepsin II Purification. Plasmepsin II was prepared according to the procedure developed by Westling et al. (*15*) and optimized for high yield and enzyme stability. The enzyme was expressed using a pET 3a expression plasmid (gift from B. Dunn's laboratory) transformed into BL21-(DE3) pLysS *E. coli*. The protein was isolated as inclusion bodies and solubilized, refolded, and purified using the methods described by Hill et al. (*16*) with slight variations. Briefly, the cells were suspended in extraction buffer [10 mM Tris (pH 8.0), 20 mM $MgCl_2$, 5 mM $CaCl_2$, and 80 μg/mL DNase I] and broken with two passes through a French pressure cell ($\geq$16000 psi). Inclusion bodies were purified by centrifugation as follows. Ruptured cells were centrifuged at 12000*g* for 30 min at 4 °C. Pellets containing inclusion bodies were resuspended in 10 mM Tris (pH 8.0), 1 mM EDTA, 2 mM 2-ME, and 100 mM NaCl and spun at 12000*g* for 30 min at 4 °C. Pellets were resuspended in 5 mM Tris (pH 8.0), 5 mM EDTA, 5 mM 2-ME, and 0.5% Triton X-100 and spun at 12000*g* for 15 min at 4 °C. Next, pellets were resuspended in 5 mM Tris (pH 8.0), 5 mM EDTA, and 5 mM 2-ME and spun as described above. Inclusion bodies were resuspended in TE buffer to a final concentration of 50 mg/mL. To refold the protein, the inclusion bodies were first denatured by dissolving them in 8 M urea, 5 mM CAPS (pH 10.5), 5 mM EDTA, and 200 mM 2-ME to a final concentration of 1 mg/mL while stirring slowly, and then dialyzed extensively against 20 mM Tris (pH 8.0) at room temperature. Any precipitated protein was pelleted at 40000*g* for 30 min at 4 °C. Soluble, folded plasmepsin II was applied directly to an anion exchange Q-Sepharose column (Q-Sepharose HP, Pharmacia) previously equilibrated with 20 mM Tris (pH 8.0). After being extensively washed, the protein was eluted by a linear gradient of 0 to 1 M NaCl in the same buffer.

Plasmepsin II Activation. The plasmepsin II precursor is autocatalyzed into the mature form under acidic conditions (*16*). The plasmepsin II precursor was dialyzed overnight against 1 L of 10 mM sodium formate buffer (pH 4.0) at 4 °C and analyzed by SDS−PAGE to ensure completion of activation. The activated protein was prepared fresh each time prior to an experiment.

Spectrophotometric Enzymatic Assays. The specific activity of plasmepsin II preparations was measured by following the hydrolysis of the chromogenic substrate Ala-Leu-Glu-Arg-Thr-Phe-nPhe-Ser-Phe-Pro-Thr-OH (California Peptide Research Inc., Napa, CA). Protease was added to a 150 μL microcuvette containing substrate at 25 °C. Final concentrations in the Michaelis−Menten assay were 400 nM plasmepsin II, 0−233 μM substrate, 10 mM sodium formate, and 2% DMSO (pH 4.0). The decrease in absorbance upon hydrolysis of the substrate was monitored at 300 nm using a Cary 100 spectrophotometer (Varian Instruments). An extinction coefficient for the absorbance difference upon hydrolysis of 1736 M^{-1} cm^{-1} at 300 nm was used to convert the absorbance change to reaction rates. Hydrolysis rates were obtained from the initial portion of the data, where at least 80% of the substrate remains uncleaved. Typical protease preparations hydrolyzed the chromogenic substrate at 2.0 $\pm$ 0.6 s^{-1} at 25 °C.

Inhibition constants (K_i) were obtained at 25 °C by measuring the rate of substrate hydrolysis using 400 nM protease in 10 mM sodium formate (pH 4.0), 163 μM substrate, and 2% DMSO with increasing amounts of inhibitor. Inhibition constants (K_i) were estimated by fitting the data to standard equations for tight binding competitive inhibitors.

Differential Scanning Calorimetry. The heat capacity function of plasmepsin II was measured as a function of temperature with a high-precision VP-DSC differential scanning calorimeter (Microcal Inc., Northampton, MA). Protein and buffer solutions were properly degassed and carefully loaded into the cells to avoid bubble formation. Exhaustive cleaning of the cells was undertaken before each experiment. Thermal denaturation scans were performed with freshly prepared plasmepsin II (20 μM) in 10 mM sodium formate (pH 4.0) and 2% DMSO. When appropriate, thermal stability measurements were also performed in the presence of increasing amounts of inhibitors. Analysis of the data was performed using software developed in this laboratory.

Isothermal Titration Calorimetry. Isothermal titration calorimetry experiments were carried out using a high-precision VP-ITC titration calorimeter system (Microcal Inc.). Since plasmepsin II aggregates and denatures under the stirring conditions of the microcalorimeter cell, standard titrations could not be performed. Instead, binding enthalpies were obtained by injecting plasmepsin II [dissolved in 10 mM sodium formate (pH 4.0) and 2% DMSO] into the microcalorimeter reaction cell containing an excess concentration of inhibitor. The heat of reaction was obtained by

injecting 10 μL of plasmepsin II (100 μM) into an inhibitor solution (30 μM) dissolved in the same buffer. The heat evolved after each injection was obtained from the time integral of the calorimetric signal. The heat of dilution was obtained by injecting 10 μL of plasmepsin II (100 μM) into the same buffer solution without the inhibitor. The heat due to the binding reaction between the inhibitor and enzyme was obtained as the difference between the heat of reaction and the corresponding heat of dilution. Under these conditions, the binding enthalpy is equal to the binding reaction heat divided by the amount of protein injected.

Determination of Antimalarial Activity. Activity was determined by measuring the level of incorporation of [^{3}H]-hypoxanthine, as described by Posner et al. (*17*). Briefly, chloroquine-sensitive *P. falciparum* cells (NF54) were maintained in a 2.4% suspension of type O^+ human erythrocytes in RPMI 1640, supplemented with 25 mM HEPES, 27 mM $NaHCO_3$, and 10% heat-inactivated human type O^+ serum, under 3% O_2, 4% CO_2, and 93% N_2. Stock solutions (20 mM) of KNI-764, KNI-840, and KNI-727 were prepared in DMSO. DMSO solutions were diluted 500-fold in medium and serially diluted in 0.2% DMSO in medium, from which 100 μL aliquots were pipetted into microtiter plate wells. Provisional EC_{50} values were obtained in a survey of ten 5-fold dilutions yielding final concentrations (in quadruplicate) of 0.00001−20 μM. Plates included eight wells of no drug controls (four with and four without DMSO) and four wells in uninfected erythrocytes. Parasite culture (0.25% parasitemia in 2.3% hematocrit, 100 μL per well) was added, and the plate was incubated for 48 h prior to the addition of 0.6 μCi of [^{3}H]hypoxanthine and a subsequent 20 h incubation. Cells were harvested onto GF-C glass filters. The filters were washed four times with 3 mL of water per sample spot, dried under a heat lamp, and counted in scintillation cocktail.

Decays per minute values were downloaded and analyzed (Microsoft Excel 5.0), to yield the mean and standard deviation at each drug concentration. Dose−response curves were fit to the experimental data by means of the Marquardt algorithm, solved for the drug concentration that kills 50% of the parasites, and analyzed for goodness of fit (R^2).

Structural Docking of KNI-727 into Plasmepsin II. The structure of KNI-727 was generated using CS Chem3D Pro (Cambridge Software) and minimized with the MM2 force field implemented in the same program. The minimized structure of KNI-727 was docked into the structure of plasmepsin II extracted from the complex of this protein with pepstatin A (PDB entry 1sme). The initial structure for the complex between plasmepsin II and KNI-727 was generated by placing the minimized structure of the inhibitor in the active site of the protein so that the hydroxyl group of KNI-727 occupied the same position as that of pepstatin A in the crystallographic structure. In all available crystallographic structures of pepstatin analogues and KNI inhibitors with aspartic proteases, these groups are positioned between the two catalytic aspartic groups (*7*, *8*). The docking of the inhibitor was carried out using the "fixed docking" option in the Affinity module of Insight II (MSI, San Diego, CA) and the CVFF force field for docking and scoring. Several independent docking simulations were carried out considering both a rigid ligand and binding site. In some simulations, the ligand and binding site were relaxed between docking steps and minimized with 100 iterations of the conjugate gradient algorithm.

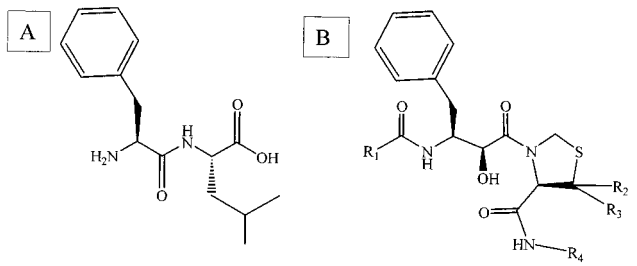

FIGURE 1: Chemical structures of the Phe−Leu dipeptide, the cleavage motif of plasmepsin II, and the allophenylnorstatine scaffold indicating the places where different chemical functional groups can be introduced.

RESULTS AND DISCUSSION

Allophenylnorstatine Scaffold. The natural substrate of plasmepsin II is hemoglobin, and within the hemoglobin molecule, the primary cleavage site is the peptide bond between Phe 33 and Leu 34 in the α chain (*18*). Accordingly, the structure of the Phe−Leu dipeptide can be used as the starting point for the development of substrate-based peptidomimetic inhibitors. As shown in Figure 1, the Phe−Leu dipeptide is significantly structurally and chemically similar to the allophenylnorstatine scaffold. Allophenylnorstatine-based compounds have been shown to be potent peptidomimetic protease inhibitors with excellent bioavailability and low toxicity (*9*−*14*). The allophenylnorstatine scaffold contains four different positions (labeled R1−R4 in the structure in Figure 1) where different chemical functional groups can be introduced to improve binding affinity and selectivity toward the selected target. Using the standard enzymatic nomenclature, the allophenylnorstatine moiety in these compounds corresponds to the P1 position, R1 corresponds to the P2 position, the thioproline group together with R2 and R3 corresponds to the P1′ position, and R4 corresponds to the P2′ position.

Figure 2 shows the chemical structure of the 12 allophenylnorstatine-based compounds considered in these studies. These compounds present a combination of different functionalities at the R1−R4 positions and provide a way of evaluating chemical preferences in the target site. The KNI series of inhibitors incorporate an allophenylnorstatine (Apns) moiety with a hydroxymethylcarboxamide (HMC) isostere at their P1 site. KNI-529 is the only exception with the anti diastereoisomer Pns [phenylnorstatine is (2*R*,3*S*)-3-amino-2-hydroxy-4-phenylbutyric acid] replacing Apns (*19*). The P1′ site is occupied by either (*R*)-1,3-thiazolidine-4-carboxylic acid (Thz) or (*R*)-5,5-dimethyl-1,3-thiazolidine-4-carboxylic acid (Dmt). The P1−P1′ moiety mimics the transition state of a substrate during the amide hydrolysis by an aspartic protease. In the case of human cathepsin D, Thz is preferred at this location. In the library used against plasmepsin II, Thz is present in KNI-357, -547, -391, -576, -272, and -529 and Dmt is present in KNI-727, -577, -413, -549, -764, and -840 (*20*, *21*). KNI-529 and -272 are tripeptide-mimetic compounds with *tert*-butylamine at their P2′ site and methylthioalanine at their P2 site. Both compounds have an isoquinolinyloxyacetyl (iQoa) at the P3 position. KNI-549 contains dimethyl and carboxyl groups at the P2 position

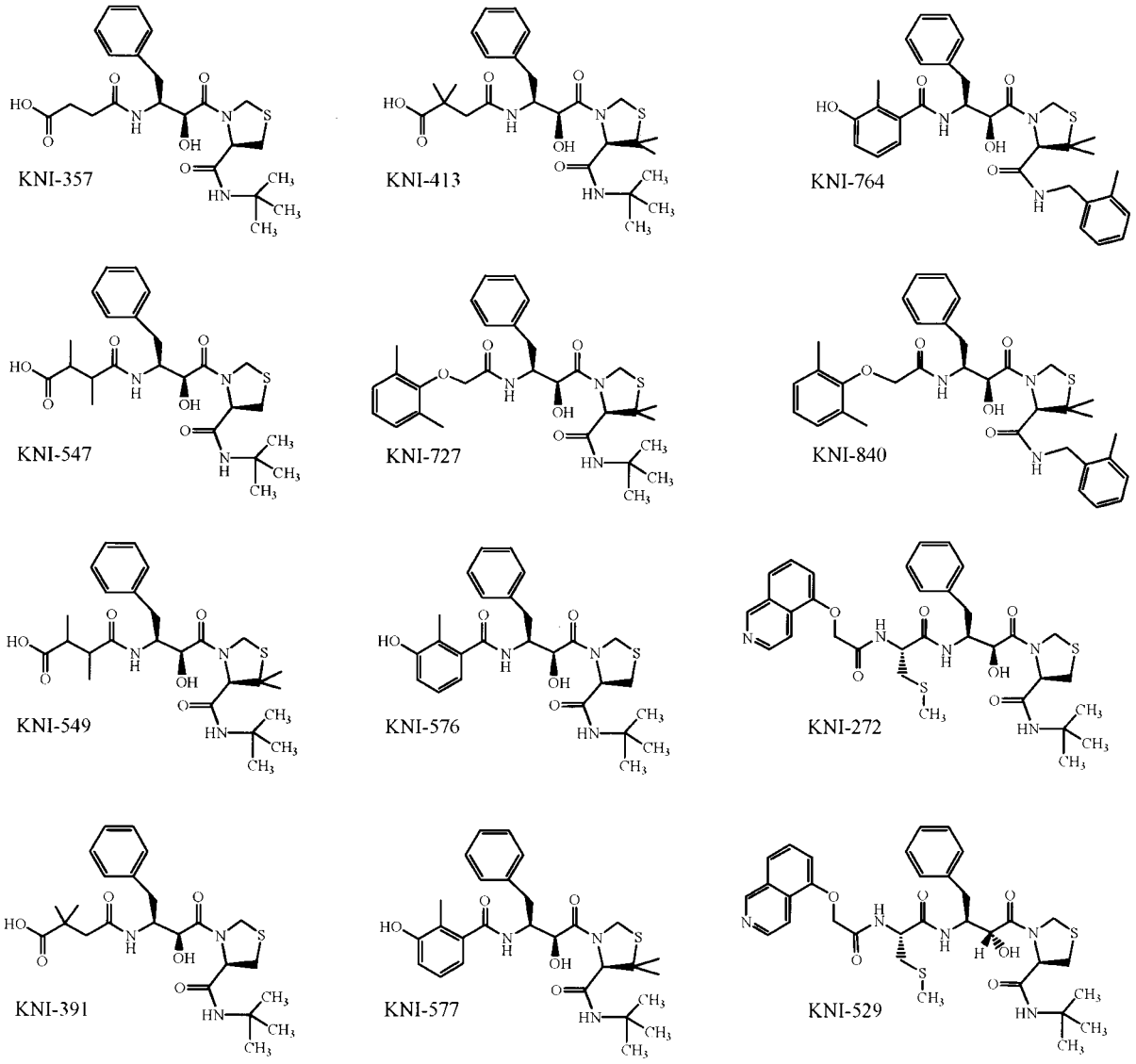

FIGURE 2: Chemical structure of the 12 allophenylnorstatine-based compounds considered in these studies.

and *tert*-butylamine at its P2′ site. KNI-577 is based on cyclyzing the P2 moiety in KNI-549. KNI-357, -547, -391, -413, -727, and -576 all contain *tert*-butylamine at their P2′ site. KNI-357 has a hydrophilic carboxyl group at its P2 position (*12*, *20*). This position is substituted with β,β-dimethyl groups in the case of KNI-391, and α,β-dimethyl groups in KNI-547. Further modification of the P2 moiety includes the introduction of the bulky and hydrophobic dimethylphenoxyacetyl in the case of KNI-727 (*11*−*13*). KNI-840 incorporates both the 2-methylbenzylamine in P2′ and dimethylphenoxyacetyl in P2 (*21*).

Enzymatic Assays. The enzymatic activity of plasmepsin II was measured with the chromogenic substrate Ala-Leu-Glu-Arg-Thr-Phe-nPhe-Ser-Phe-Pro-Thr-OH under conditions that mimic the acidic environment found in the digestive vacuole of the parasite (*2*). In 10 mM sodium formate (pH 4.0) and 2% DMSO at 25 °C, a K_m of 40 ± 10 μM and a k_{cat} of 2.0 ± 0.6 s^{-1} were obtained. These values remained essentially unchanged when the experiments were repeated in the presence of 0.1 M NaCl [10 mM sodium citrate, 0.1 M NaCl (pH 4.0), and 2% DMSO at 25 °C]. In this case, a K_m of 48 ± 4 μM and a k_{cat} of 2.6 ± 0.4 s^{-1} were obtained. These values are comparable to parameters previously reported by Westling (*22*) and Hill (*23*). The enzymatic activity of human cathepsin D was measured against the same substrate under similar solvent and temperature conditions. For this enzyme, the kinetic data yielded a K_m of 96 ± 40 μM and a k_{cat} of 2.5 ± 0.5 s^{-1} in 10 mM sodium formate (pH 4.0) and 2% DMSO at 25 °C. In the presence of 0.1 M NaCl, these values were 136 μM and 3.1 ± 0.7 s^{-1} for K_m and k_{cat}, respectively.

Enzyme inhibition assays were performed with both plasmepsin II and cathepsin D. Table 1 presents the results of the analysis. The inhibition constants (K_i) of the KNI compounds against plasmepsin II ranged between 0.02 and 97 μM and for cathepsin D between 0.08 and 38 μM. The best plasmepsin II inhibitor in the series is KNI-840; however, it has only a 4-fold selectivity with respect to cathepsin D. KNI-727 has a slightly higher K_i (0.07 μM) but a 22-fold selectivity with respect to cathepsin D. Another compound with high affinity was KNI-764 (0.03 μM), but it exhibited only a 7-fold discrimination against cathepsin D. Overall, the best compound is KNI-727, in terms of both plasmepsin II affinity and cathepsin D selectivity. Figure 3 illustrates the kinetic data obtained with KNI-727, for both plasmepsin II and cathepsin D. Inspection of the structure−

Table 1: Inhibition Constants of Allophenylnorstatine-Based Compounds against Plasmepsin II and Cathepsin D

compound	MW	K_i for plasmepsin II (μM)	K_i for cathepsin D (μM)	selectivity
KNI-840	604	0.02 ± 0.01	0.08 ± 0.09	4.1
KNI-764	576	0.03 ± 0.009	0.2 ± 0.02	6.7
KNI-727	555	0.07 ± 0.04	1.6 ± 0.3	22.4
KNI-577	527	0.6 ± 0.07	3.4 ± 0.7	5.8
KNI-272	667	1.0 ± 0.2	2.6 ± 0.3	2.6
KNI-413	521	1.4 ± 0.5	7.3 ± 1.4	5.2
KNI-529	667	8.1 ± 2.6	8.8 ± 2.8	1.1
KNI-549	521	8.6 ± 1.3	37.7 ± 8.20	4.4
KNI-576	499	9.3 ± 3.6	7.0 ± 1.6	0.8
KNI-391	493	12.7 ± 1.5	1.4 ± 0.08	0.1
KNI-547	493	30.7 ± 8.1	18.2 ± 3.3	0.6
KNI-357	466	96.9 ± 19.1	8.1 ± 1.5	0.08

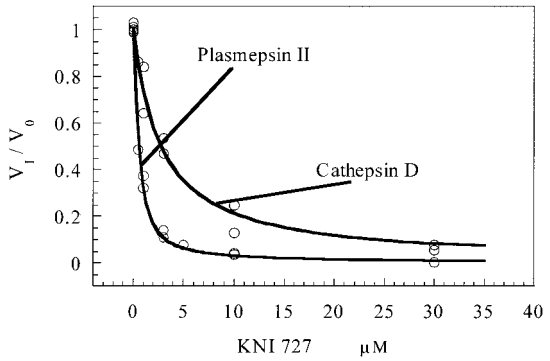

FIGURE 3: Normalized inhibition kinetics data obtained with KNI-727, for both plasmepsin II and cathepsin D.

activity profile suggests that dimethylphenoxyacetyl may be good at the P2 position, allophenylnorstatine at P1, and dimethylthioproline at P1′. Similarly, the presence of the *tert*-butylamide at P2′ apparently reduces the affinity toward cathepsin D significantly. Since KNI-727 is the best lead compound, a detailed thermodynamic analysis of the binding energetics of this compound was performed by isothermal titration calorimetry and differential scanning calorimetry.

Thermodynamic Analysis of Plasmepsin II and KNI-727 Binding. The binding affinity of an inhibitor (K_a) is determined by the Gibbs energy of binding (ΔG) which in turn is determined by the enthalpy (ΔH) and entropy (ΔS) changes ($\Delta G = \Delta H - T\Delta S$). In principle, many combinations of ΔH and ΔS values can give rise to the same ΔG value and, therefore, elicit the same binding affinity. However, enthalpically dominated ligands do not behave the same as entropically dominated ligands. It has been recently shown that enthalpic inhibitors are preferable because they do not require extremely large entropy changes to achieve high binding affinity (*24*−*26*). Since a large favorable entropy change arises from a combination of a large gain in solvent entropy and a minimal loss of conformational entropy, these compounds tend to be extremely hydrophobic and rigid, lacking the ability to efficiently adapt to changes in the target or to be effective against naturally occurring polymorphisms. Accordingly, a rigorous dissection of the binding affinity of KNI-727 into its enthalpic and entropic components was performed.

The enthalpy of binding of KNI-727 to plasmepsin II was measured directly by isothermal titration calorimetry (ITC). The results of the experiments are shown in Figure 4. In these experiments, the heat effects associated with the addition of a small amount of enzyme to the ITC reaction cell containing a large excess of inhibitor are measured. Conventional titrations in which small aliquots of the inhibitor are added to the reaction cell containing plasmepsin II could not be performed because plasmepsin II has a tendency to aggregate and denature under the prolonged stirring conditions in the calorimeter cell. The experimental protocol in Figure 4 does not include prolonged stirring of the protein. These experiments yielded a binding enthalpy (ΔH_a) of −4.4 ± 0.3 kcal/mol at 25 °C.

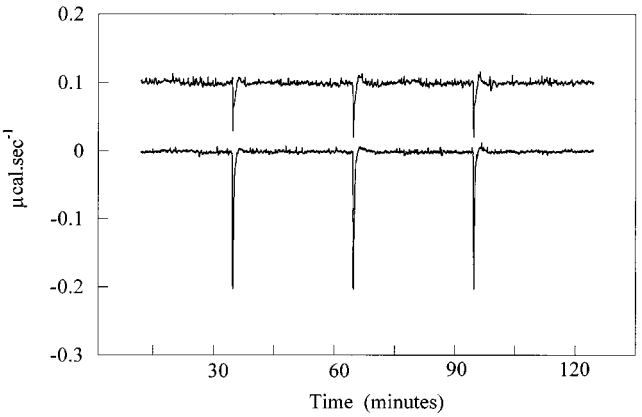

FIGURE 4: Determination of the enthalpy of binding of KNI-727 to plasmepsin II by isothermal titration calorimetry. In these experiments, an excess concentration of inhibitor (30 μM) is placed in the calorimeter reaction cell. At predetermined time intervals, 10 μL of a 100 μM plasmepsin II solution is injected into the reaction cell (bottom trace). The heat of dilution is obtained by injecting the same protein solution into the reaction cell containing only buffer (top trace). The enthalpy of binding is obtained by subtracting the heat of dilution from the heat measured in the experiments with protein and inhibitor. The experiments were performed in 10 mM sodium formate and 2% DMSO (pH 4.0).

The thermodynamic analysis indicates that KNI-727 binds to plasmepsin II with a Gibbs energy ($\Delta G = \Delta H - T\Delta S$) of −9.96 kcal/mol at 25 °C in a process which is almost equally favored by enthalpic (ΔH = −4.4 kcal/mol) and entropic ($-T\Delta S$ = −5.56 kcal/mol) interactions. This enthalpy−entropy balance is a very desirable property in lead compounds and greatly facilitates subsequent optimization (*24*, *26*). In general, the incorporation of enthalpically favorable interactions is always difficult in molecular design, and consequently, enthalpically favorable lead compounds provide a better starting point for subsequent optimization since manipulation of entropy contributions either by changes in hydrophobicity or by the introduction of conformational constraints is easier to implement (*26*).

The accuracy of the binding parameters was validated by their ability to predict inhibitor-induced changes in the structural stability of plasmepsin II. These experiments were performed by utilizing high-sensitivity differential scanning calorimetry (DSC). Figure 5 shows the excess heat capacity function of plasmepsin II at different concentrations of the inhibitor KNI-727. In the absence of inhibitor, plasmepsin II is characterized by a denaturation temperature of 63.3 °C, which increases to higher temperatures as the inhibitor concentration is increased. In the absence of inhibitor, the denaturation enthalpy is equal to 162 kcal/mol and the heat capacity change is equal to 4.8 ± 0.5 kcal K^{-1} mol^{-1}. Figure 6 shows the dependence of the denaturation temperature, T_m,

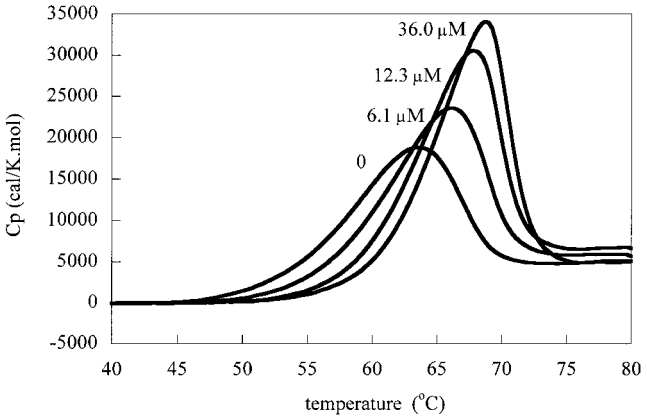

FIGURE 5: Excess heat capacity function of plasmepsin II at different concentrations of the inhibitor KNI-727. The calorimetric scans were performed in 10 mM sodium formate (pH 4.0) and 2% DMSO. Only four scans are shown for presentation purposes.

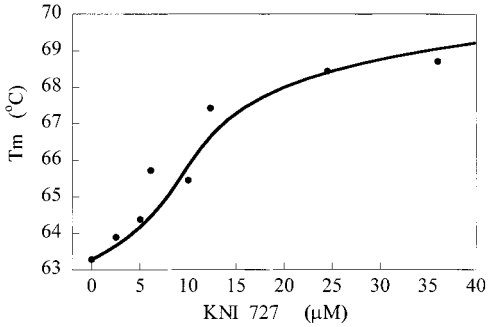

FIGURE 6: Dependence of the denaturation temperature, T_m, of plasmepsin II on the concentration of KNI-727. The solid line is the theoretical line predicted by the linkage equations for protein stability and binding and the thermodynamic parameters obtained calorimetrically. See the text for details.

on the concentration of KNI-727. In the presence of the inhibitor, the structural stability of plasmepsin II is modified according to the equation

$$\Delta G = \Delta G^\circ + RT \ln(1 + K_a[X]) \quad (1)$$

where ΔG° is the Gibbs energy in the absence of the inhibitor and obtained from the DSC data in the absence of the inhibitor, K_a is the binding affinity of the inhibitor, and [X] is the free inhibitor concentration. Since only the total inhibitor concentration is known, the free concentration is calculated according to the equation

$$[X] = \frac{-b + \sqrt{b^2 + 4K_a[X_T]}}{2K_a} \quad (2)$$

where $b = -K_a[X_T] + 0.5[P_T]K_a + 1$ at the temperature under which half of the protein is denatured. $[P_T]$ is the total protein concentration. The solid line in Figure 6 represents the best fit to the data and is consistent with a binding affinity of $(2.0 \pm 0.1) \times 10^7$ M^{-1} or a K_d of 0.05 μM which is very close to the K_i determined from the enzymatic inhibition assay. As seen in the figure, the calculated dependence of the denaturation temperature accurately accounts for the experimental values, consistent with a thermodynamic mechanism. The calorimetric data are also consistent with a ΔC_p of binding of -200 cal K^{-1} mol^{-1}, which is close to the value expected from a structure-based thermodynamic analysis (see below).

Structure-Based Thermodynamic Modeling of KNI-727 Binding. From a structural standpoint, the enthalpy change primarily reflects the strength of the interactions between the inhibitor and the target protein (e.g., van der Waals, hydrogen bonds, etc.) relative to those existing with the solvent. As mentioned above, the entropy change mainly reflects two contributions: changes in solvation entropy and changes in conformational entropy. After binding takes place, desolvation occurs, water is released, and a gain in solvent entropy is observed. This gain is particularly important for hydrophobic groups. At the same time, the ligand and certain groups in the protein lose conformational freedom, resulting in a negative change in conformational entropy. A common strategy for improving the binding affinity of a compound is increasing its hydrophobicity and introducing conformational constraints. This strategy makes the entropy change more favorable by increasing the solvation entropy and minimizing the loss of conformational entropy of the inhibitor upon binding. When this approach is applied to lead compounds that are already enthalpically favorable, the probability of developing extremely high-affinity inhibitors is significantly increased (*26*). However, this approach requires a dissection of enthalpic contributions so that chemical modifications can be targeted to regions that are not contributing significantly to the binding enthalpy.

To investigate the origin of the favorable binding enthalpy of KNI-727, computational studies aimed at docking the inhibitor into the crystallographic structure of plasmepsin II bound to pepstatin A (PDB entry 1sme) were performed. Several independent docking simulations (both with and without minimization between docking steps) rendered structures consistent with a binding mode similar to that observed for pepstatin A. In particular, the hydroxyl group in the allophenylnorstatine moiety of KNI-727 remains within hydrogen bonding distance of the two catalytic aspartic residues and the backbone of the KNI inhibitor adopts a structure very similar to that of pepstatin A. The side chains of the inhibitor occupy the same subsites as the side chains of pepstatin A, despite the bulkiness of some of the substituents in the KNI-727 structure. In the predicted structure, KNI-727 establishes potential hydrogen bond interactions with the protein backbone and with polar side chains (Figure 7). These interactions will contribute to the favorable binding enthalpy observed experimentally. The application of the structural parametrization of the energetics (*27*−*29*) to the model structure results in a predicted binding enthalpy of -4.9 kcal/mol, which is close to the experimental value. According to the structural modeling results, KNI-727 is predicted to interact strongly with residues in the catalytic region of plasmepsin II as well as with residues in the flap. Figure 7 indicates the location of the plasmepsin II residues that interact most strongly (>0.2 kcal/mol) with the inhibitor. Residues are color coded according to the strength of the interaction (blue for the strongest interaction and red for no interaction). Correspondingly, residues Asp 34, Gly 36, Asp 214, Gly 216, Thr 217, Ser 218, Leu 131, and Tyr 192 define a binding hot spot in the catalytic region of the binding site, while residues Asn 76, Tyr 77, and Val 78 define a second one in the flap. The interactions of the

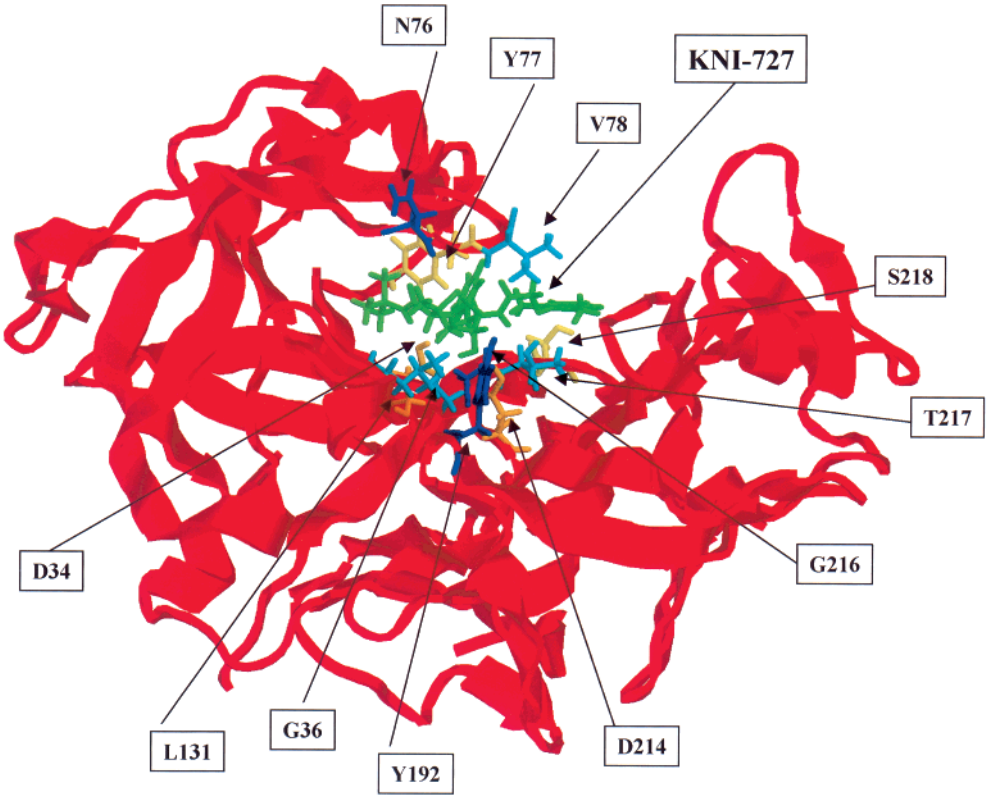

FIGURE 7: Docking of KNI-727 (green) into the plasmepsin II structure. Protein residues have been colored according to their predicted interaction with the inhibitor (blue for the strongest interaction and red for no interaction). Amino acids predicted to interact strongly with the inhibitor are depicted using a stick representation.

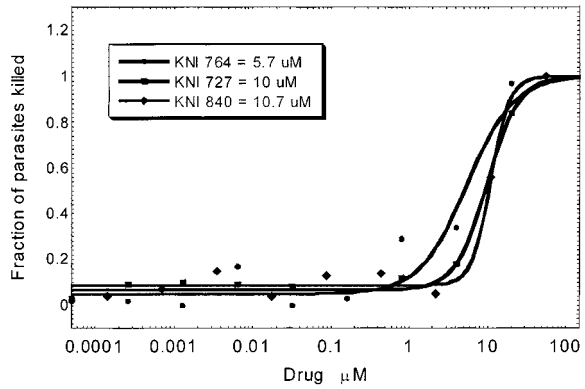

FIGURE 8: Results of cytotoxicity assays in the erythrocytic *P. falciparum*, chloroquine-sensitive NF54 strain for KNI-764, KNI-727, and KNI-840.

inhibitor with residues in the catalytic region are predicted to contribute most of the favorable binding enthalpy, suggesting that optimization of this compound must preferably involve the introduction or modification of functional groups that target the flap region or the edges of the binding pocket.

Plasmodium-Infected Red Blood Cell Assays. Cytotoxicity assays in the erythrocytic *P. falciparum* chloroquine-sensitive NF54 strain (*30*, *31*) were performed for the top three compounds (KNI-764, KNI-727, and KNI-840). The results are shown in Figure 8 and are consistent with EC_{50}s of 5.7, 10, and 10.7 μM for KNI-764, KNI-727, and KNI-840, respectively. Previously, Ellman et al. (*32*) described compounds with EC_{50}s of 2−10 μM (*32*). These compounds, however, have low selectivity toward plasmepsin II over cathepsin D. Silva et al. (*8*) studied a panel of linear and cyclic compounds containing a modified statine motif (*8*). The best compound in this panel inhibited the growth of *P. falciparum* only up to 54% with 20 μM inhibitor. Recently, Jiang et al. (*33*) identified diphenylurea derivatives that inhibited plasmepsin II with K_i values ranging between 1 and 6 μM. Since some diphenylurea derivatives as well as allophenylnorstatine derivatives have been identified before as HIV-1 protease inhibitors, it is apparent that the large reservoir of compounds developed during the course of HIV-1 protease inhibition research can provide starting libraries for the development of inhibitors against other important proteases. For KNI-727, there is an ~100-fold difference between the in vitro K_i and the EC_{50} measured in cell assays. Differences of this kind have been observed before for other drug therapies, including HIV-1 protease inhibitors currently in clinical use, and are usually attributed to inhibitor binding to serum proteins, albumin, and α_1-acid glycoprotein (see, for example, ref *34*).

CONCLUSIONS

The combined effect of strong inhibition of plasmepsin II, high selectivity against cathepsin D, and good inhibition of parasite growth in erythrocyte cultures indicates that allophenylnorstatine provides an attractive scaffold for developing powerful inhibitors with potential clinical applications as antimalarials. Another attractive characteristic of these compounds is that they exhibit good oral bioavailability and low toxicity. From the point of view of molecular optimization, a significant feature of these compounds is that they inhibit plasmepsin II with a favorable enthalpy change and therefore offer the possibility for the incorporation of

functional groups aimed at achieving extremely tight binding affinities. This will be the subject of a future communication.

ACKNOWLEDGMENT

To Dr. Theresa Shapiro from the Department of Pharmacology, Johns Hopkins University School of Medicine (Baltimore, MD), for performing the red blood cell assays. To Dr. Daniel Goldberg and Dr. Ben Dunn for providing us with plasmepsin II plasmids.

REFERENCES

1. Wyler, D. J. (1993) *Clin. Infect. Dis. 16*, 449−458.
2. Francis, S. E., Sullivan, D. J., and Goldberg, D. E. (1997) *Annu. Rev. Microbiol. 51*, 97−123.
3. Butler, D., Maurice, J., and O'Brien, C. (1997) *Nature 386*, 535−541.
4. Miller, L. H., Good, M. F., and Milon, G. (1994) *Science 264*, 1878−1883.
5. Goldberg, D. E. (1993) *Semin. Cell Biol. 4*, 355−361.
6. Francis, S. E., Banerjee, R., and Goldberg, D. E. (1997) *J. Biol. Chem. 272*, 14961−14968.
7. Luker, K. E., Francis, S. E., Gluzman, I. Y., and Goldberg, D. E. (1996) *Mol. Biochem. Parasitol. 79*, 71−78.
8. Silva, A. M., Lee, A. Y., Gulnik, S. V., Majer, P., Collins, J., Bhat, T. N., Collins, P. J., Cachau, R. E., Luker, K. E., Gluzman, I. Y., Francis, S. E., Oksman, A., Goldberg, D. E., and Erickson, J. W. (1996) *Proc. Natl. Acad. Sci. U.S.A. 93*, 10034−10039.
9. Kiso, Y. (1996) *Biopolymers 40*, 235−244.
10. Kiso, Y. (1998) *J. Synth. Org. Chem. 56*, 32−43.
11. Kiso, Y., Yamaguchi, S., Matsumoto, H., Mimoto, T., Kato, R., Nojima, S., Takaku, H., Fukazawa, T., Kimura, T., and Akaji, K. (1998) *Arch. Pharm. Pharm. Med. Chem. 331*, 87−89.
12. Kiso, Y., Matsumoto, H., Mizumoto, S., Kimura, T., Fujiwara, Y., and Akaji, K. (1999) *Biopolymers 51*, 59−68.
13. Mimoto, T., Kato, R., Takaku, H., Nojima, S., Terashima, K., Misawa, S., Fukazawa, T., Ueno, T., Sato, H., Shintani, M., Kiso, Y., and Hayashi, H. (1999) *J. Med. Chem. 42*, 1789−1802.
14. Mimoto, T., Hattori, N., Takaku, H., Hisanuki, S., Fukazawa, T., Terashima, K., Kato, R. Y., Nojima, S., Misawa, S., Ueno, T., Imai, J., Enomoto, H., Tanaka, S., Sakikawa, H., Shintani, M., Hayashi, H., and Kiso, Y. (2000) *Chem. Pharm. Bull. 48*, 1310−1326.
15. Westling, J., Yowell, C. A., Mayer, P., Erickson, J. W., Dame, J. B., and Dunn, B. M. (1997) *Exp. Parasitol. 87*, 185−193.
16. Hill, J., Tyas, L., Phylip, L. H., Kay, J., Dunn, B. M., and Berry, C. (1994) *FEBS Lett. 352*, 155−158.
17. Posner, G. H., Gonzalez, L., Cumming, J. N., Klinedinst, D., and Shapiro, T. (1997) *Tetrahedron 53*, 37−50.
18. Goldberg, D. E., Slater, A. F. G., Beavis, R., Chait, B., Cerami, A., and Henderson, G. B. (1991) *J. Exp. Med. 173*, 961−969.
19. Katoh, E., Yamazaki, T., Kiso, Y., Wingfield, T. T., Stahl, S. J., Kaufman, J. D., and Torchia, D. A. (1999) *J. Am. Chem. Soc. 121*, 2607−2608.
20. Matsumoto, H., Matsuda, T., Nakata, S., Mitoguchi, T., KImura, T., Hayashi, Y., and Kiso, Y. (2001) *Bioorg. Med. Chem. 9*, 417−430.
21. Matsumoto, H., Kimura, T., Hamawaki, T., Kumagai, A., Goto, T., Sano, K., Hayashi, Y., and Kiso, Y. (2001) *Bioorg. Med. Chem. 9*, 1589−1600.
22. Westling, J., Cipullo, P., Hung, S.-H., Saft, H., Dame, J. B., and Dunn, B. M. (1999) *Protein Sci. 8*, 2001−2009.
23. Hill, J., Tyas, L., Phylip, L. H., Kay, J., Dunn, B. M., and Berry, C. (1994) *FEBS Lett. 352*, 155−158.
24. Velazquez-Campoy, A., Todd, M. J., and Freire, E. (2000) *Biochemistry 39*, 2201−2207.
25. Velazquez-Campoy, A., Todd, M. J., Vega, S., and Freire, E. (2001) *Proc. Natl. Acad. Sci. U.S.A. 98*, 6062−6067.
26. Velazquez-Campoy, A., Kiso, Y., and Freire, E. (2001) *Arch. Biochem. Biophys. 390*, 169−175.
27. Luque, I., Gomez, J., Semo, N., and Freire, E. (1998) *Proteins 30*, 74−85.
28. Velazquez-Campoy, A., Luque, I., and Freire, E. (2001) *Thermochim. Acta 380*, 217−227.
29. Leavitt, S., and Freire, E. (2001) *Curr. Opin. Struct. Biol. 11*, 560−566.
30. Desjardins, R. E., Canfield, C. J., Haynes, J. D., and Chulay, J. D. (1979) *Antimicrob. Agents Chemother. 16*, 710−718.
31. Bodley, A. L., Cumming, J. N., and Shapiro, T. A. (1998) *Biochem. Pharmacol. 55*, 709−711.
32. Haque, T. S., Skillman, G., Lee, C. E., Habashita, H., Gluzman, I. Y., Ewing, T. J. A., Goldberg, D. E., Kuntz, I. D., and Ellman, J. A. (1999) *J. Med. Chem. 42*, 1428−1440.
33. Jiang, S., Prigge, S. T., Wei, L., Gao, Y. E., Hudson, T. H., Gerena, L., Dame, J. B., and Kyle, D. E. (2001) *Antimicrob. Agents Chemother. 45*, 2577−2584.
34. Molla, A., Vasavanonda, S., Kumar, G., Sham, H. L., Johnson, M., Grabowski, B., Denissen, J. F., Kohlbrenner, W., Plattner, J. J., Leonard, J. M., Norbeck, D. W., and Kempf, D. J. (1998) *Virology 250*, 255−262.

BI0117549